

Chapter 6

Short-Readout Spiral Imaging

Spiral MR imaging has many desirable properties, and is an efficient technique allowing for relatively fast image acquisition. As gradient performance improves, it is important to reconsider the design of fast sequences to best make use of new hardware. This chapter examines the design of fast spiral imaging sequences to use the CV/i or “cardiovascular” gradients designed for GE systems. A tradeoff between very fast imaging and very short readout times is shown, allowing short scan times with little off-resonance effects. Two applications of short-readout spiral imaging are discussed—multi-phase, multi-slice imaging for bolus perfusion measurements and rapid three-dimensional imaging.

6.1 Motivation

Spiral imaging trajectories have excellent properties for imaging flowing blood [86], largely due to their low first moments compared with EPI or standard 2DFT imaging trajectories [87]. Additionally, the sampling of the k -space center on every readout helps to reduce artifacts from pulsatile flow.

The goal here is to use spiral trajectories for rapid imaging of 3D volumes. Previous authors have used a stack-of-spirals trajectory, shown in Fig. 6.1, mostly for

imaging coronary arteries [88–91]. Individual 2D spiral readouts are designed for new high-performance gradient systems, using short readout times where the gradient heating limits match pulse-duration limits on repetition time. The shortened readout times reduce the effects of off-resonance and T_2 or T_2^* blurring and allow for short-repetition sequences such as steady-state free precession (SSFP) and spoiled gradient-recalled echo (SPGR). SSFP imaging gives a “ T_2/T_1 ” contrast that provides a bright fluid signal, and can be useful for angiography, neurological imaging or imaging of joints. SPGR generates T_1 contrast that is often used for T_1 quantification including contrast-enhanced perfusion measurements.

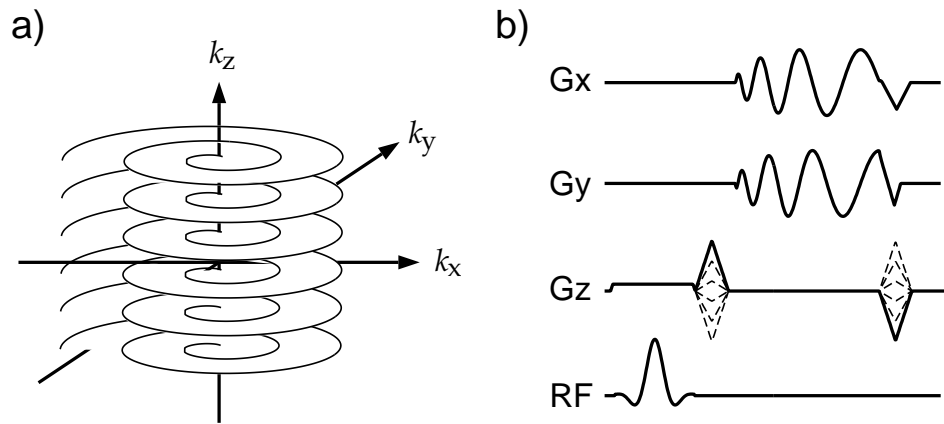


Figure 6.1: The stack-of-spirals k -space trajectory (a) is created by the pulse sequence shown in (b). Spiral readouts in k_x and k_y , with phase-encoding in k_z , provide efficient coverage of 3D k -space.

6.2 Spiral Design for Fast Gradient Amplifiers

There are many different types of spiral trajectory that can be used for imaging. The Archimedian spiral, for which the radius is directly proportional to the amount of turning has the desirable property that the k -space density is fairly uniform. Design of these gradient waveforms has been addressed previously [92, 93], using

circuit models for the gradients. The simple method used here uses fixed limits on gradient amplitudes and slew rates, resulting in slightly longer readouts.

6.2.1 Spiral Trajectory Design

The design of spiral trajectories has several constraints. First, hardware constraints limit the maximum gradient amplitude and slew rate. For interleaved spiral imaging, the starting angle of the trajectory must be variable, meaning that the gradient *vector* magnitude and slew rate *vector* magnitude are constrained. Second, FOV limitations put a limit on the rate of increase in the radial direction compared with the rate of turning, and also the maximum gradient vector magnitude.

For a 2D spiral it is useful to express the k -space location, gradient and slew rate as complex vectors. The desired Archimedian spiral trajectory can be described as

$$\mathbf{k} = a\theta e^{i\theta} \quad (6.1)$$

where $\mathbf{k} = k_x + ik_y$. The parameter a determines the rate of increase in the radial direction with respect to the rate of turning, and for a uniform density spiral,

$$a = \frac{N\Delta k_{max}}{2\pi} = \frac{N}{2\pi FOV} \quad (6.2)$$

where N is the number of spiral interleaves, and Δk_{max} is the maximum sample spacing for the Nyquist limit.

The design problem then becomes how to choose θ as a function of time so as to remain within the other constraints. First, differentiation of Eq. 6.1 gives

$$\mathbf{G} = \frac{2\pi a}{\gamma} e^{i\theta} (\dot{\theta} + i\theta\dot{\theta}) \quad (6.3)$$

Differentiation again gives the expression for the slew-rate vector, where $\dot{\theta}$ and $\ddot{\theta}$ are the first and second derivatives of θ with respect to time:

$$\mathbf{S} = \frac{2\pi a}{\gamma} e^{i\theta} \left[(\ddot{\theta} - \theta\dot{\theta}^2) + i(2\dot{\theta}^2 + \theta\ddot{\theta}) \right] \quad (6.4)$$

Equations 6.3 and 6.4 have been shown previously [93, 94]. Hardware constraints limit $|\mathbf{G}|$ and $|\mathbf{S}|$ to G_{max} and S_{max} respectively. Furthermore, Nyquist sampling constrains the gradient magnitude as $|\mathbf{G}| \leq \frac{2\pi}{\gamma\tau FOV}$, where τ is the sampling period. The lower of the two limits $|\mathbf{G}|$ is used.

Now θ can be designed as a function of time iteratively. At first, θ and $\dot{\theta}$ are both 0, and the trajectory is slew-rate limited. Equation 6.4 is solved for $\ddot{\theta}$ given the slew-rate limit. Next, $\dot{\theta}$ and θ are obtained from (discrete) integration of $\ddot{\theta}$. The iteration loop then steps: these values are used to calculate the next value of $\ddot{\theta}$ that is in turn integrated to give $\dot{\theta}$ and θ .

As the gradient magnitude grows, it eventually reaches its limit. At this point, Eq. 6.3 can be solved to give $\dot{\theta}$, which is integrated to give θ . As a check, $\ddot{\theta}$ can be calculated from discrete differentiation of $\dot{\theta}$ and used with Eq. 6.4 to check that the slew limit is not reached. In practice, once the gradient limit is reached, the uniform-density spiral remains gradient-limited for its entire duration.

This iterative calculation repeats until a given k -space radius is reached. Alternatively, the length of the readout could be limited instead. Either way, the design must usually be repeated a few times to achieve the desired combination of readout length, FOV, number of interleaves and resolution.

For most methods, it is desirable to rewind the spiral gradients. There are many ways to do this “optimally,” though using simple trapezoidal waveforms and limiting each axis independently to $\frac{1}{\sqrt{2}}$ of its maximum amplitude and slew rate achieves close to the optimal rewinder speed. In some cases it is useful to rewind the first moment of the gradients as well [95].

A sample spiral design is shown in Fig. 6.2. The k -space trajectory (Fig. 6.2a) is a uniform-density spiral that can be shown parametrically by the k_x and k_y waveforms (Fig. 6.2b). The gradient and slew-rate waveforms (Figs. 6.2c and d) show the portions of the readout that are gradient and slew-rate limited respectively.

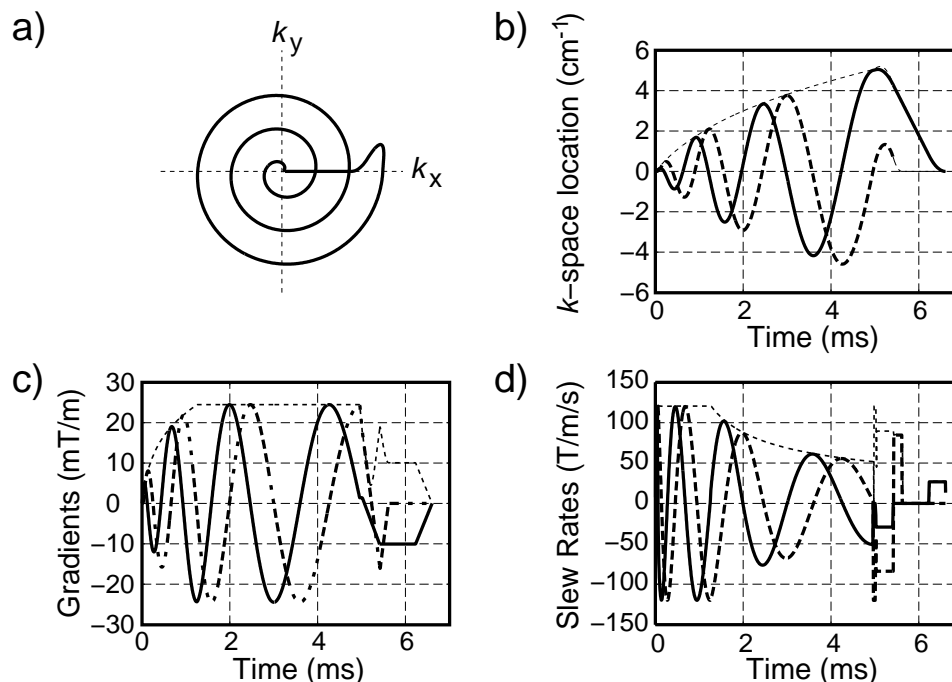


Figure 6.2: Sample of spiral gradient waveform design, showing k -space trajectory (a), and time plots of the waveforms k (b), G (c) and S (d). In (b-d), the solid, dashed and dotted lines correspond to the x-component, y-component and magnitude of each vector.

Variable-density spiral waveforms can be calculated using a similar method by allowing the parameter a to vary with k -space radius. Equations 6.3 and 6.4 will then vary with k -space, but the general formulation can still be used.

6.2.2 Gradient Heating Considerations

Aside from gradient amplitude and slew-rate limitations, gradient amplifier heating can limit the gradient duty cycle. A heating model for the scalable gradient drivers (SGDs) used in the GE CV/i gradients has been shown [96]. The model calculates energy based on gradient amplitude, square of gradient amplitude, and amplitude during which the gradient is slewing. The average power generated by heating is

then reduced by limiting the gradient duty cycle. If the cumulative energy produced by heating is divided by maximum safe power dissipation, the result is the minimum time needed to dissipate that cumulative energy. This is shown in Fig. 6.3, which shows the minimum dissipation time as a function of progression along the gradient, broken down by the three heat energy sources described above. This minimum-dissipation time is the minimum sequence repetition time.

Figure 6.3 shows that the dominant source of heat is the period during which the gradient is slewing. This heat term is proportional to the integral of gradient amplitude during this time. Since a certain gradient-amplitude integral is required to reach the desired k -space radius, an effective way to reduce the heating is by reducing the period of slewing itself. Spiral gradient designs with a reduced amount of slewing have been shown, both for reduction of heating [97] and for use on scanners capable of only piece-wise linear gradient waveforms [98].

For a given FOV and resolution, the number of interleaves, N , can be varied. Both the minimum TR and the readout time decrease as the number of interleaves is increased. However, since an increasing amount of time is spent at the k -space center as N increases, the total scan time actually increases slightly as shown in Fig. 6.4. Additionally, as N increases, the amount of dead time per TR necessary to satisfy heating constraints decreases. When this dead time is less than the duration of non-readout pulses such as excitation and phase encoding pulses, the scan time begins to increase rapidly with N as Fig. 6.4 shows.

Short readouts are advantageous because off-resonance effects, and T_2 and T_2^* effects are reduced. Additionally, shorter repetition times are possible with steady-state free precession imaging (Section 6.4.1). For this reason, given a desired FOV and resolution, and a certain duration for the excitation pulse, the number of interleaves is chosen at the “knee” in the plot in Fig. 6.4a [99].

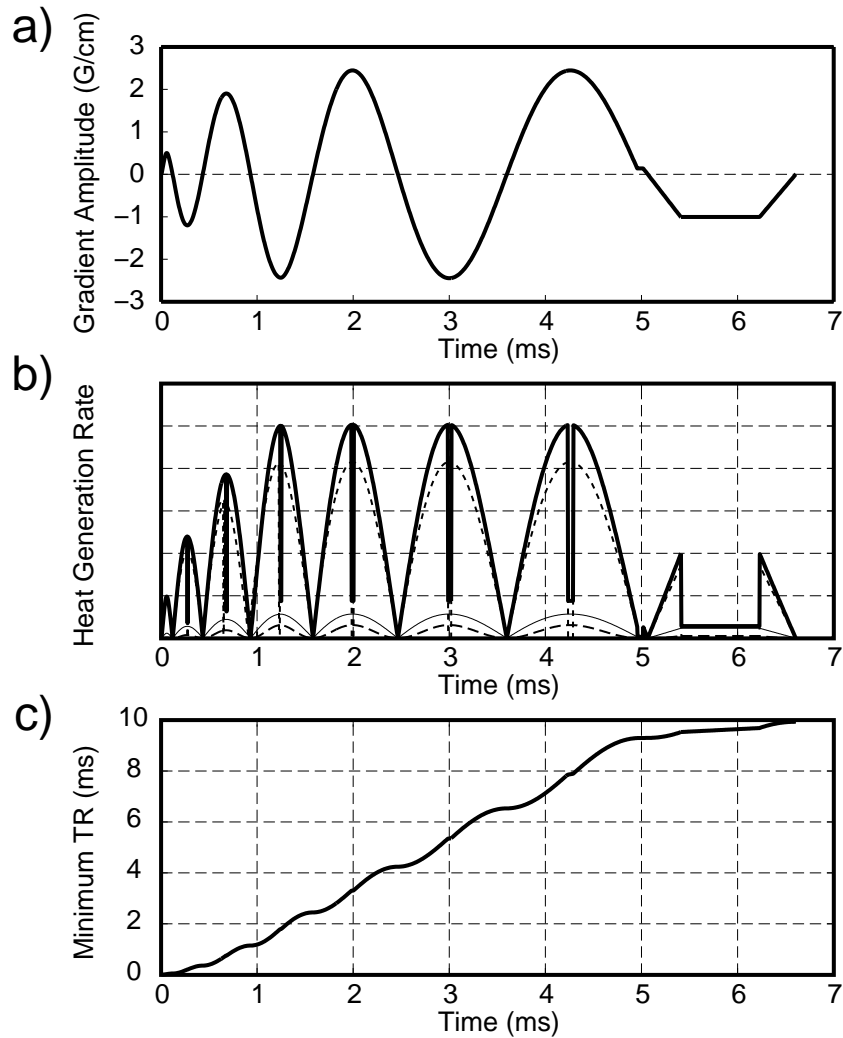


Figure 6.3: Accrual of time needed for dissipation of heat produced in gradient amplifiers. A typical spiral gradient waveform is shown in (a). The three heat sources proportional to gradient amplitude, square of amplitude, and amplitude while slewing are shown by thin solid, dashed and dotted lines respectively in (b), with the total heat produced shown by the thick solid line. Finally, the time needed to safely dissipate the total power produced by each source is plotted as a function of the time along a gradient waveform (c).

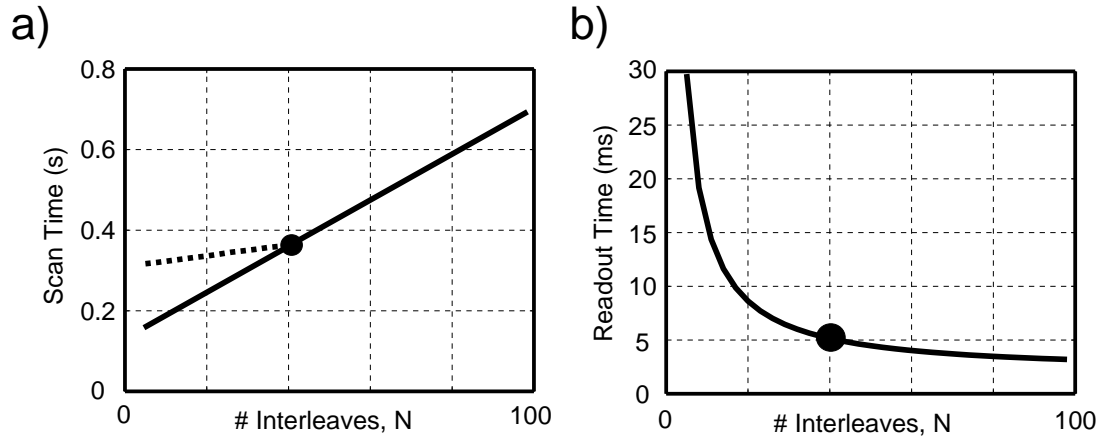


Figure 6.4: Scan time (a) and readout duration (b) plotted as a function of the number of interleaves, N . The scan time is limited by heating constraints (dotted line) for low N , and by the pulse durations (excitation plus readout) for higher N . As N increases, the readout duration decreases. The black dots on each plot represent the point the choice of N used based on (a). This is a reasonable tradeoff between reducing scan time and reducing readout duration.

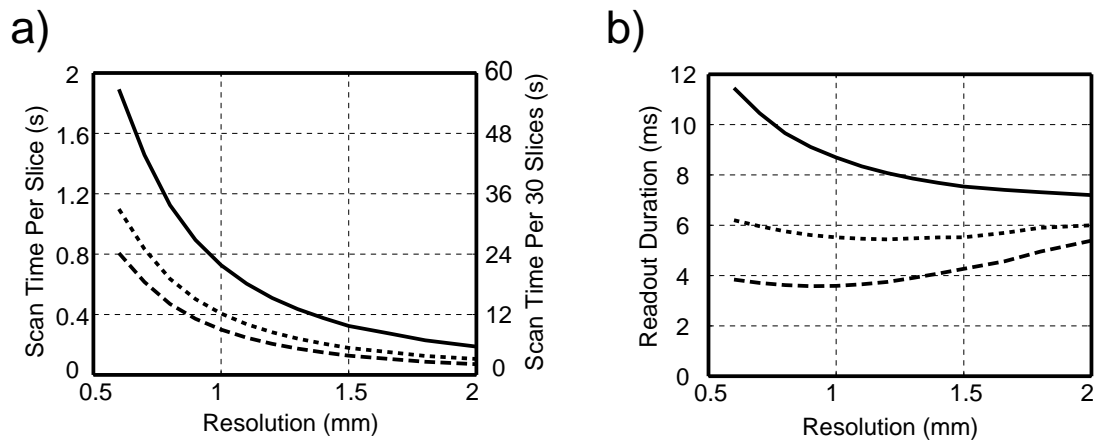


Figure 6.5: Time-per-slice and per-30-slices (a) and readout duration (b) plotted as a function of resolution for different FOV. In each case, the number of interleaves is chosen at the “knee” of Fig. 6.4. The solid, dotted and dashed lines represent a FOV of 36 cm, 24 cm and 12 cm respectively.

6.3 Image Reconstruction

Sampling along a spiral trajectory complicates the image reconstruction, since the data do not lie on a grid. A standard method called gridding [100] interpolates the non-Cartesian data onto a Cartesian grid. A fast Fourier transform (FFT) can then be used to reconstruct the image.

When a stack-of-spirals trajectory is used the gridding process is separable in the xy and z directions. The data in each k -space plane may be gridded separately before or after the FFT in the phase-encoded direction. The GE scanner used for these experiments performs this FFT before the raw data are stored, so the reconstruction algorithm is identical for 3D or multi-slice reconstruction.

6.4 Imaging Applications

Short readouts have the advantage that short-repetition-time sequences can be used, particularly SPGR and SSFP. SSFP can be used to provide “ T_2/T_1 ” contrast for fast 3D imaging or angiography. SPGR is used to provide T_1 contrast in contrast-enhanced perfusion imaging.

6.4.1 Ultrafast 3D SSFP Imaging and Angiography

The 3D stack-of-spirals sequence implemented using fully-refocused gradients (Fig. 6.1) provides a refocused-SSFP sequence with a fairly short repetition time, and readout durations of about 6 ms. For a 24 cm FOV, 1 mm resolution, and 40 interleaves, a TR of 10 ms was achievable. A partial- k -space acquisition was used in some cases by acquiring 60% of the phase-encodes ($k_x - k_y$ planes) and using a homodyne reconstruction [55].

In refocused-SSFP imaging, as was discussed in Section 4.3.1, the signal is highly sensitive to variations in resonant frequency, resulting in a banding artifact. The artifact can be shifted in frequency by incrementing the phase of successive RF

excitation pulses. By using multiple acquisitions with different increment amounts, a flat spectral response is artificially obtained by simply taking the maximum signal at each pixel over all acquisitions [70].

Several different scan parameter combinations were used to acquire images. First an axial slab with $24 \times 24 \times 12 \text{ cm}^3$ and $1 \times 1 \times 2 \text{ mm}^3$ resolution was acquired using a 30° tip-angle and partial stack-of-spirals. To reduce the SSFP banding artifact, acquisitions with two and four RF phase cycles were acquired [70, 71]. An image from each of these acquisitions is shown in Fig. 6.6.

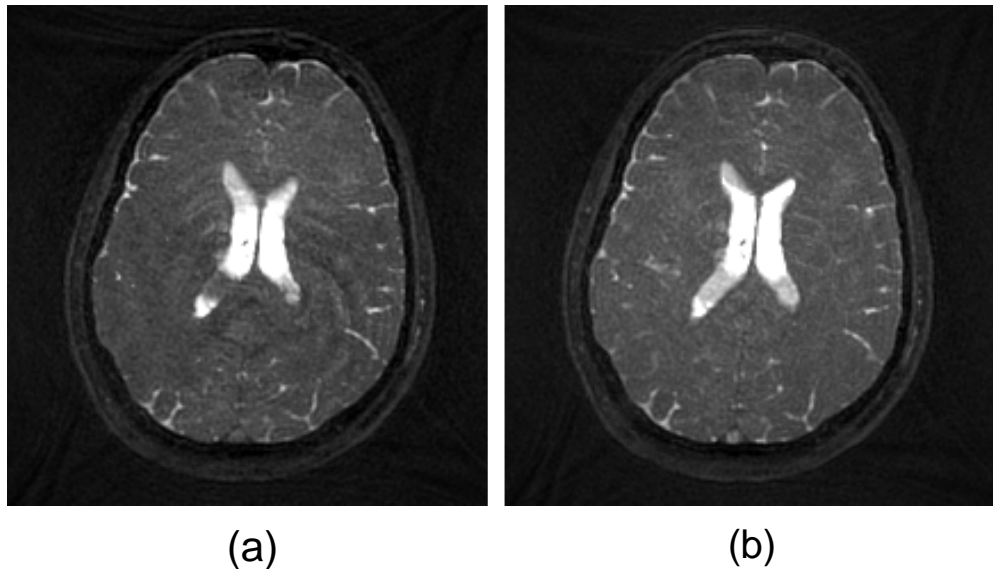


Figure 6.6: Axial slices from 3D SSFP acquisitions using partial stack-of-spirals using two RF phase cycles for a 23 s scan time (a) and four RF phase cycles for a 47 s scan time (b).

The brain images shown in Fig. 6.6 show high SNR and very good contrast between cerebrospinal fluid (CSF) and other brain tissue. The “ T_2/T_1 ” contrast of SSFP does not provide much contrast between grey matter and white matter. In the brain, the use of two RF phase cycles appears to provide sufficient reduction of the SSFP banding artifact. Registration of the multiple acquisitions may be a problem with this method, but could be solved by using much shorter repetition

times as presented recently by Meyer et al. [95]. Although the grey-white matter contrast may limit the practical value of this method for imaging of the brain, the 23 second scan time is very encouraging.

As a second application of this sequence, 3D images of the lower leg vasculature were acquired, again using an axial slab with $24 \times 24 \times 12 \text{ cm}^3$ and $1 \times 1 \times 2 \text{ mm}^3$ resolution. A tip angle of 60° was used to maximize contrast between arterial blood and muscle. Images using partial- k -space and full- k -space acquisitions and using two and four RF phase cycles were acquired using an extremity transmit-receive coil.

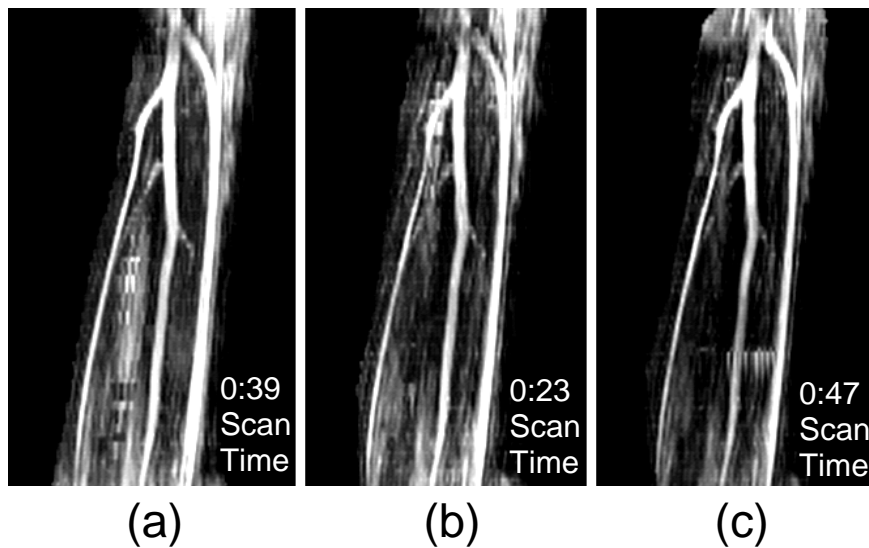


Figure 6.7: Targeted maximum-intensity-projections from 3D SSFP acquisitions of the lower leg of a normal volunteer showing the popliteal artery trifurcation. The acquisitions use 2 RF phase cycles and full k -space (a), 2 RF phase cycles and 60%- k -space (b), and 4 RF phase cycles and full k -space (c). The scan times were 39 s, 23 s and 47 s for (a), (b) and (c) respectively.

Targeted maximum-intensity-projections (MIPs) from three different acquisitions are shown in Fig. 6.7. All three images show bright signal from the popliteal artery. The large flip angle helps to suppress signal from muscle and venous blood. The targeted MIPs were necessary to remove the high bone marrow signal from the

projections. The three images are comparable in quality, though the SNR of the full- k -space image (a) is slightly higher than the other two images.

This method shows that 3D flow-independent angiograms are achievable in very short scan times. However, again, registration of multiple acquisitions may present a problem. Additionally, nulling the first-moment of all gradient waveforms between RF excitation pulses would enhance the signal from flowing tissue, as discussed in [95]. The repetition time could be further decreased by using a shorter excitation pulse. A final improvement for angiography, particularly in the body would be fat-suppression. Fat-suppressed refocused-SSFP images have recently been shown by Scheffler and Hennig [80], and by Block *et al.* [101] using linear-combination SSFP [71].

6.4.2 Continuous Multi-Slice Imaging for Contrast-Enhanced Perfusion

A final application of short-readout spiral imaging is contrast-enhanced perfusion, which was presented by Kaji *et al.* [102]. The short readouts allow interleaved multi-slice SPGR imaging with temporal resolution of about 1.1 s for 4 slices with 24×24 cm² FOV and 1.25×1.25 mm² resolution. The slices are spread across the lower leg, with about 7 cm between slices. Following injection of a contrast agent, images were acquired continuously for 60 s, enough time for perfusion to the lower leg musculature. The T_1 -contrast of SPGR enables calculation of the perfusion to the tissue, shown in Fig. 6.8.

6.5 Summary

Two-dimensional spiral readout trajectories offer a very efficient imaging method that has excellent flow and motion properties. For three-dimensional imaging, a stack-of-spirals maintains most of these advantages. As gradient hardware has improved, the spiral waveforms have been improved to allow a balance between fast

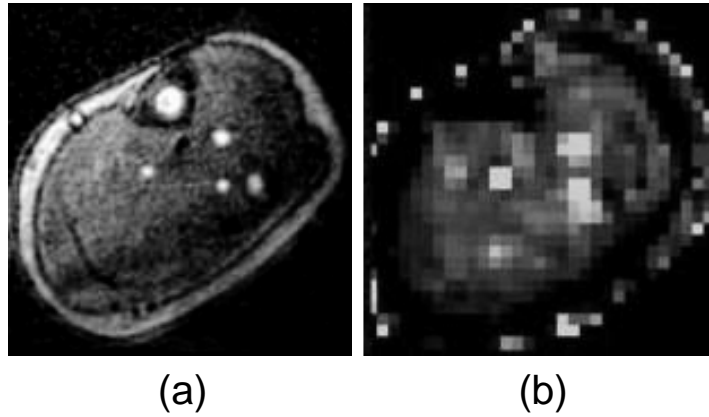


Figure 6.8: The T_1 -contrast of SPGR in a time series of spiral images of the lower leg (a) can be used to calculate a perfusion map (b). The brightness of the perfusion map indicates the amount of perfusion to tissue across the image.

imaging and short readouts. The short readouts allow interleaved multi-slice SPGR imaging with a short repetition-time as well as refocused-SSFP imaging for rapid 3D imaging and angiography.